

Macrocyclization in the Design of Grb2 SH2 Domain-Binding Ligands Exhibiting High Potency in Whole-Cell Systems

Chang-Qing Wei,[†] Yang Gao,[†] Kyeong Lee,[†] Ribo Guo,[‡] Bihua Li,[‡] Manchao Zhang,[‡] Dajun Yang,[‡] and Terrence R. Burke, Jr.,^{*,†}

Laboratory of Medicinal Chemistry, Center for Cancer Research, National Cancer Institute—Frederick, National Institutes of Health, Frederick, Maryland 21702, and Department of Hematology/Oncology, University of Michigan Medical School, Ann Arbor, Michigan 48109

Received August 22, 2002

While most SH2 domains bind phosphotyrosyl (pTyr) containing peptides in extended fashion, the growth factor receptor-bound protein 2 (Grb2) SH2 domain preferentially binds ligands in bend conformations. Accordingly, incorporation of bend-inducing functionality into synthetic ligands could potentially enhance their affinity for this SH2 domain. A macrocyclic tripeptide mimetic that contains a simplified pTyr surrogate lacking an α -nitrogen has recently been shown to exhibit high Grb2 SH2 domain-binding affinity in extracellular ELISA-based assays. However, the same compound is largely ineffective in whole-cell assays. It is known that acidic functionality originating from the α -nitrogen of pTyr residues or from the α -position of P⁰ pTyr mimetics not only increases binding affinity of peptides to Grb2 SH2 domains in extracellular assays but also enhances potency in cell-based systems. Such functionality is absent from the previously reported macrocycle. Therefore, the current study was undertaken to examine the effects of introducing carboxylic functionality at the pTyr mimetic α -position of macrocyclic ligands. It was found that such a modification not only enhanced Grb2 SH2 domain binding in extracellular assays but also conferred high efficacy in whole-cell systems. The most potent compound of the current study exhibited an IC₅₀ value of 0.002 μ M in an extracellular ELISA-based assay, and in MDA-MB-453 cells, it both inhibited the association of Grb2 with p185^{erbB-2} and exhibited antimitogenic effects with submicromolar IC₅₀ values.

Introduction

Overactivation of growth factor protein tyrosine kinase (PTK) pathways can promote cellular proliferation and metastasis and thereby contribute to the etiology of human cancers.¹ Down regulation of pathogenic PTK signaling by kinase inhibitors affords a new and potentially noncytotoxic approach toward anticancer therapy.^{2–5} Src homology 2 (SH2) domains play important roles in PTK signaling pathways, and SH2 domain-binding antagonists potentially represent complementary alternatives to PTK inhibitors as new therapeutics for treatment of a variety of diseases.^{6–9} Of numerous families of SH2 domains, the growth factor receptor-bound protein 2 (Grb2) SH2 domain is included among those considered to be attractive targets for antagonist development.^{10,11} On the basis of the preferential binding of Grb2 SH2 domains to pY–X–N-containing sequences in type I β -bend conformations,¹² scientists at Novartis Corporation developed a variety of high-affinity Grb2 SH2 domain-binding tripeptides that incorporate a bend-inducing α -aminocyclohexylcarboxylic acid residue (Ac₆C) in the pTyr + 1 position.¹³ The naphthylpropylamido-containing **1** is representative of this class of compound (Figure 1).¹⁴ In a followup study, replacement of pTyr with the hydrolytically stable

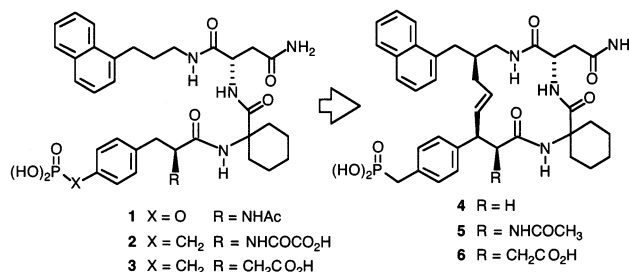


Figure 1. Macrocyclization in the design of phosphatase-stable Grb2 SH2 domain-binding ligands.

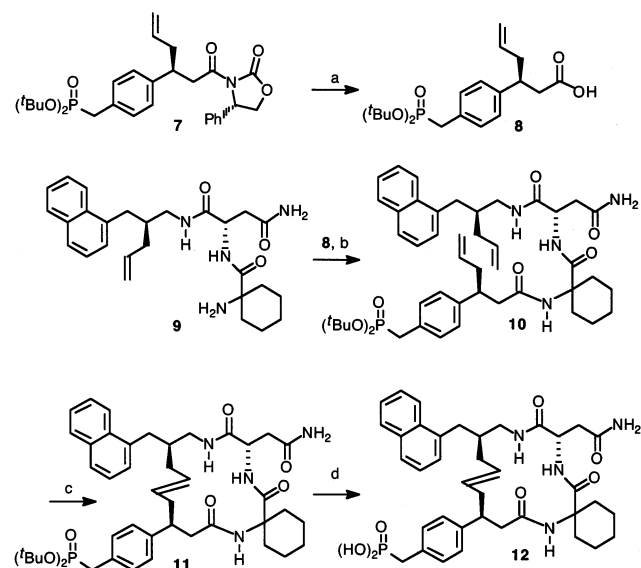
phosphonomethylphenylalanine (Pmp) residue bearing an *N*^ε-oxalyl residue (compound **2**) was reported as a variant of **1** that displayed enhanced antagonism of Grb2 SH2 domain binding in cellular assays.¹⁵ More recently, the α -carboxymethyl analogue **3** has also been shown to exhibit good cellular efficacy.¹⁶

In a separate study, macrocycle **4** was prepared in an effort to reduce binding entropy penalties by constraining the peptide backbone of **2** to bend conformations.¹⁷ Although such a constraint would be in addition to the bend-inducing effects already afforded by the Ac₆C residue,^{18,19} it was felt that ring closure achieved by joining the β -position of the pTyr-mimicking residue to the central methylene of the *N*-terminal naphthylpropyl group could potentially achieve additional conformational benefit through side chain rotational constraint. To reduce synthetic complexity, carboxylic acid containing –NHCOCO₂H or –CH₂C O₂H functionalities at the pTyr mimetic α -positions of open-chain **2** or **3** respec-

* To whom correspondence should be addressed. Address: Laboratory of Medicinal Chemistry, Center for Cancer Research, NCI—Frederick, P.O. Box B, Building 376, Boyles Street, Frederick, MD 21702-1201. Phone: (301) 846-5906. Fax: (301) 846-6033. E-mail: tburke@helix.nih.gov.

[†] National Institutes of Health.

[‡] University of Michigan Medical School.

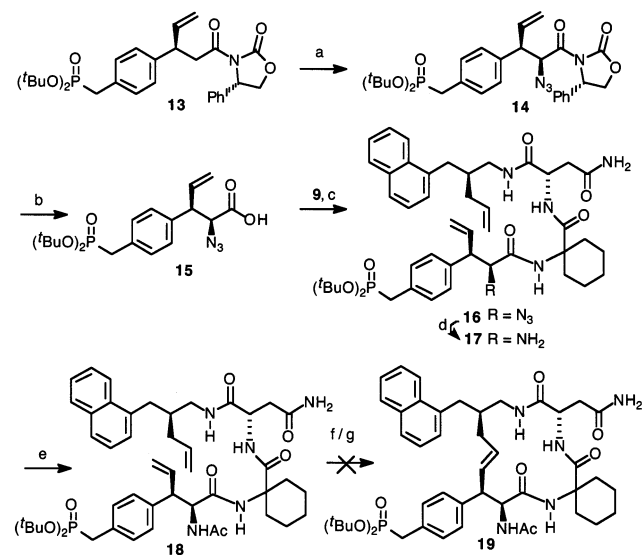
Scheme 1^a

^a Reagents and conditions: (a) H_2O_2 , LiOH, THF– H_2O , 90% yield; (b) HOBT, EDCI, DMF, 79% yield; (c) $(\text{PCy}_3)_2\text{Cl}_2\text{Ru}=\text{CHPh}$, CH_2Cl_2 , reflux, 77% yield; (d) TFA– SiEt_3 – H_2O , quantitative.

tively, were deleted from **4**.²⁰ By use of an in vitro enzyme-linked immunosorbent assay (ELISA) based binding assay, it was observed that **4** exhibited an approximate 100-fold increase in binding affinity relative to the open-chain congener.¹⁷ However, the ability of **4** to block the association of activated erbB-2 PTK with cognate Grb2 in whole cells was paradoxically less than would be expected on the basis of in vitro binding data. Additionally, attenuation of growth-factor-driven mitogenesis of MDA-MB-453 cells was also significantly reduced relative to what would have been expected.

It is known for open-chain ligands that the functionality arising from the pTyr α -position provides important binding interactions with the $\alpha\text{A}2$ Arg67 residue of the Grb2 SH2 domain.¹² The lack of equivalent functionality in macrocycle **4** could potentially reduce its in vivo efficacy. To examine the importance both in vitro and in vivo of functionality arising from the pTyr mimetic α -position and to enhance the efficacy of macrocyclic ligands, the current study was undertaken to prepare analogues of types **5** and **6**, which represent fully functionalized macrocyclized versions of the parent open-chain compounds **2** and **3**, respectively.

Synthesis. The synthesis of macrocycle **12** (Scheme 1), which represents a one-carbon ring expansion of **4**, was analogous to that used to make **4**²⁰ except that the pTyr-mimicking residue (**8**) contained an allylic group at the β -position rather than a vinyl group. Hydrolysis of Evans chiral auxiliary functionality from starting **7** (previously prepared as an intermediate in the synthesis of a pipercolic acid based pTyr mimetic²¹) provided **8**, which was coupled with known dipeptide **9**.²⁰ This gave the metathesis precursor **10**, which was ring-closed to **11** in good yield using the method of Grubbs.^{22–24} As previously reported, for both **12** and all other macrocycles contained in the current paper, stereochemistries at sites of ring juncture for both the naphthylpropyl and pTyr mimetic portions were predicated on the absolute configurations of the corresponding Evans reagents used

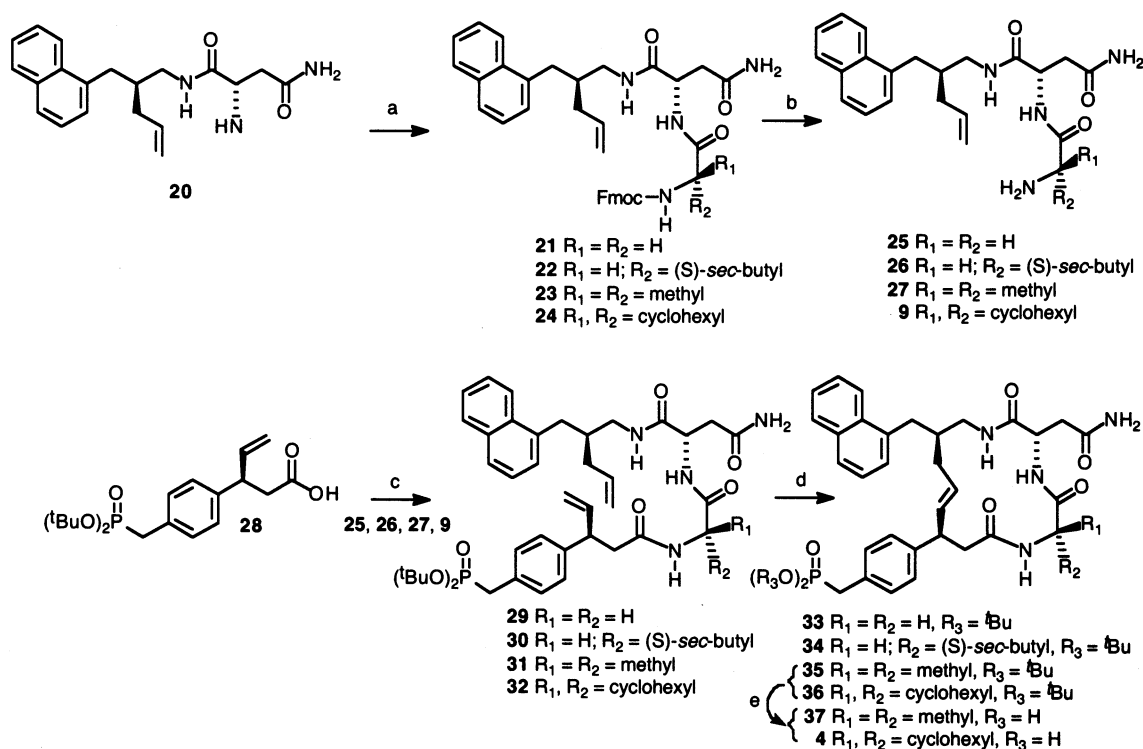
Scheme 2^a

^a Reagents and conditions: (a) NaHMDS, trisyl azide, THF, -78°C , 73% yield; (b) H_2O_2 , LiOH, THF– H_2O , 92% yield; (c) HOBT, DIPCDI, DMF, 70% yield; (d) Ph_3P , THF– H_2O , reflux, quantitative; (e) Ac_2O , Et_3N , CH_2Cl_2 , 80% yield; (f) $(\text{PCy}_3)_2\text{Cl}_2\text{Ru}=\text{CHPh}$, CH_2Cl_2 , reflux; (g) $(\text{PCy}_3)(\text{IMes})\text{Cl}_2\text{Ru}=\text{CHPh}$, toluene, 80°C .

in their synthesis.²⁰ Finally, removal of phosphonate *tert*-butyl protection provided the desired ring-expanded **12**.

Syntheses of macrocycles bearing an α -amino substituent within the pTyr-mimicking residue were attempted next. As outlined in Scheme 2, the initial approach was similar to that used to prepare parent macrocycle **4**²⁰ except that the α -azido functionality was employed as a protected, latent amine.²⁵ Accordingly, azidation of known **13**²⁰ using trisyl azide and sodium hexamethyldisilylamide (NaHMDS) gave α -azido **14** in good yield. This was then converted to the free acid **15** using standard hydrolysis conditions. Coupling of **15** to dipeptide **9** using HOBT-active ester conditions provided the corresponding azido-containing tripeptide **16** (70% yield), which was reduced to the α -amino-containing **17** using triphenylphosphine in refluxing aqueous THF. Acetylation using acetic anhydride gave metathesis precursor **18**. Unexpectedly, ring closure to **19** could not be accomplished using either standard Grubbs catalyst $[(\text{PCy}_3)_2\text{Cl}_2\text{Ru}=\text{CHPh}]$ ²⁶ or a more recently reported second-generation catalyst 4,5-dihydroimidazol-2-ylidene-substituted ruthenium-based catalyst $[(\text{PCy}_3)(\text{IMes})\text{Cl}_2\text{Ru}=\text{CHPh}]$.²⁷

Since failure of ring closure might be due to steric crowding by the $\text{Ac}_{6\text{C}}$ residue, ring closure was attempted with open-chain precursors in which the cyclohexane portion of the $\text{Ac}_{6\text{C}}$ residue had been replaced by less bulky groups (**29–31**, Scheme 3). In initial studies, these open-chain precursors lacked functionality in the pTyr mimetic α -position. Synthesis of requisite open-chain analogues **29–31**, as well as $\text{Ac}_{6\text{C}}$ -containing **32**, began by HOBT-active ester coupling of appropriate commercially available *N*-Fmoc amino acids, Gly, Ile, α -amino isobutyric acid and α -cyclohexane carboxylic acid, with known asparagine amide **20**²⁰ to give the corresponding dipeptides **21–24**, respectively. Deprotection (piperidine in DMF) yielded the free amines **25–27** and **9**, which were coupled in good yield with known

Scheme 3^a

^a Reagents and conditions: (a) for **21**, Fmoc-Gly-OH, HOBT, DIPCPI, DMF, 89% yield; for **22**, Fmoc-Ile-OH, HOBT, DIPCPI, DMF, 86% yield; for **23**, Fmoc-Aib-OH, HOBT, DIPCPI, DMF, 88% yield; for **24**, Fmoc-1-amino-cyclohexane carboxylic acid, HOBT, DIPCPI, DMF, 82% yield; (b) piperidine, DMF, quantitative; (c) HOBT, DIPCPI, DMF, 81% yield (**29**); 81% yield (**30**); 78% yield (**31**); 76% yield (**32**); (d) (PCy₃)₂Cl₂Ru=CHPh, CH₂Cl₂, reflux, 63% yield (**35**); 67% yield (**36**); (e) TFA-SiEt₃-H₂O, quantitative.

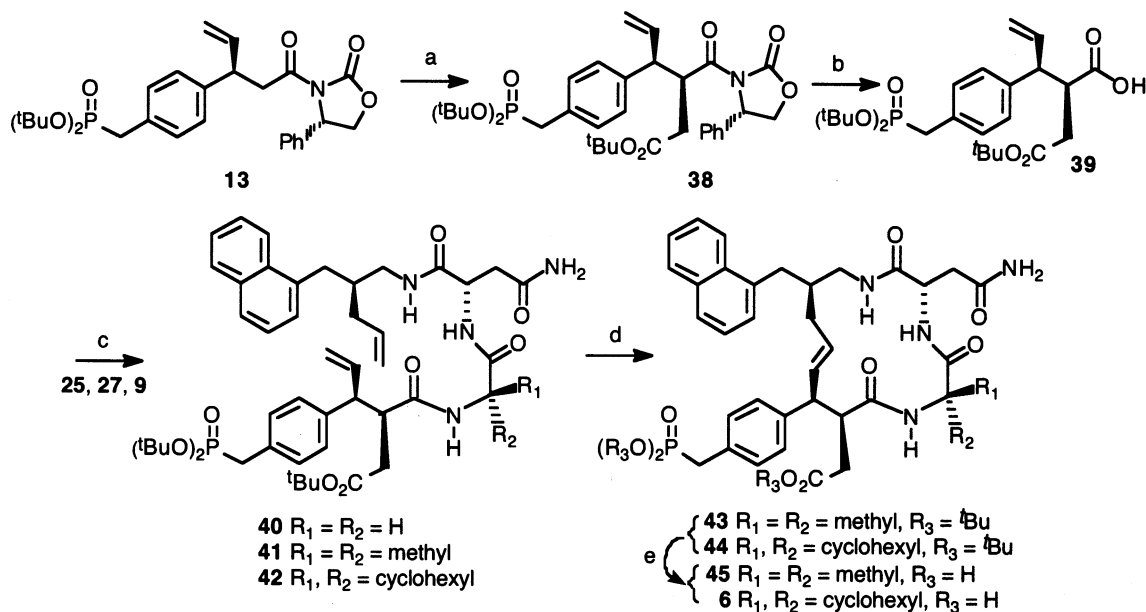
β -vinyl-containing desamino analogue **28**²⁰ to provide the desired olefin metathesis precursors **29**–**32**. Attempted synthesis of macrocycles **33** and **34** by olefin metathesis ring closure of **29** and **30**, respectively, failed despite repeated attempts. Alternatively, ring closure of **31** proceeded in good yield to provide macrocycle **35**, as did ring closure of **32** to yield **36**, consistent with the previous synthesis of this latter compound.²⁰ Deprotection of the acidic functionality in **35** and **36** gave the desired final products **37** and **4**, respectively.

One consequence of the above study using simplified pTyr mimetics lacking α -substituents was that successful ring closure appeared to require a proximal α,α -disubstituted residue at the pTyr mimetic + 1 position. Accordingly, the fully elaborated macrocycles **45** and **6** were next prepared bearing α -carboxymethyl substituents on their pTyr mimetics (Scheme 4). The requisite *tert*-butyl-protected pTyr mimetic **39**, containing α -carboxymethyl and β -vinyl substituents, was prepared from precursor **13** by procedures similar to the synthesis of the analogous compound lacking a β -vinyl group.¹⁶ Metathesis precursors **40**, **41**, and **42** were then prepared by coupling of **39** with dipeptides **25**, **27**, and **9**, respectively. Analogue **40**, which lacked an α,α -disubstituted residue at the pTyr mimetic + 1 position was included, since it was uncertain whether introduction of the α -carboxymethyl substituents on the pTyr mimetic might induce conformational factors favoring ring closure even in the absence of the otherwise required pTyr mimetic + 1 α,α -substituents. Intramolecular ring closure of **41** and **42** yielded desired macrocycles **43** and **44**, respectively, in good yields. The geometry of the ring-closing double bond in macrocycle

44, which contains a cyclohexyl-bearing pTyr mimetic + 1 residue, was established as *E* on the basis of NMR coupling constants of the olefinic proton at δ 5.74 (dd, J = 10.1 and 14.1 Hz). This was in agreement with similar results previously obtained with compound **36** (δ 5.66; dd, J = 9.3 and 14.4 Hz). Compound **40** failed to undergo olefin metathesis, further supporting the requirement for ring closure of an α,α -disubstituted residue at the pTyr mimetic + 1 position. Finally, global hydrolysis of *tert*-butyl protection on **43** and **44** provided target macrocycles **45** and **6**, which were purified by HPLC.

Results and Discussion

Synthetic Considerations. It was unclear whether the ring-closing three-carbon bridge of parent macrocycle **4** provided the optimum ring size and geometry for binding to the Grb2 SH2 domain. Therefore, prior to undertaking introduction of the pTyr mimetic α -functionality, which was the focus of the current study, we first examined whether a larger ring size would exhibit higher affinity. This resulted in the preparation of expanded analogue **12**, which contains one additional methylene in its ring-closing segment. Unexpectedly, such a seemingly minor modification resulted in a near-total loss of binding affinity (**12**; IC₅₀ > 10 μ M; Table 1). Molecular modeling studies indicated that binding interactions of **12** differ significantly from those of **4**, which contains a three-carbon ring-closing segment. Of particular note are differences in positioning of the critical Asn side chain carboxamido groups as well as naphthyl rings, both of which are critical for tight Grb2 SH2 domain binding (Figure 2). This indicated the

Scheme 4^a

^a Reagents and conditions: (a) NaHMDS, BrCH₂CO₂Bu^t, THF, -78 °C, 77% yield; (b) LiOH, H₂O₂, THF-H₂O, 85% yield; (c) HOAt, EDCI, DMF, 85% yield (**40**), 75% yield (**41**), 72% yield (**42**); (d) (PCy₃)₂Cl₂Ru=CHPh, CH₂Cl₂, reflux, 83% yield (**43**), 87% yield (**44**); (e) TFA-SiEt₃-H₂O, quantitative.

Table 1. Inhibition Data Obtained in Extracellular ELISA-Based Grb2 SH2 Domain-Binding Assays

Compound	R	X	n =	IC ₅₀ +/- SD (μM) ^a
6	CH ₂ CO ₂ H		0	0.002 +/- 0.0003
12	H		1	>10
37	H		0	0.7 +/- 0.2
45	CH ₂ CO ₂ H		0	0.008 +/- 0.0003

^a Values were obtained as described in the Experimental Section.

importance of maintaining the original three-carbon bridge in further analogues.

On the basis of the above finding, further analogues in the study were prepared employing a three-carbon ring-closing segment. Accordingly, preparation of macrocycle **19**, bearing the acetamido functionality in the pTyr mimetic α-position, was undertaken. However, it was found that olefin-metathesis-induced ring closure of the corresponding open-chain precursor **18** could not be achieved using standard Grubbs catalyst [(PCy₃)(IMes)Cl₂Ru=CHPh] or a more recently reported second-generation catalyst [(PCy₃)(Im(Mes)₂)Ru=CHPh]. In light of the relatively facile ring closure

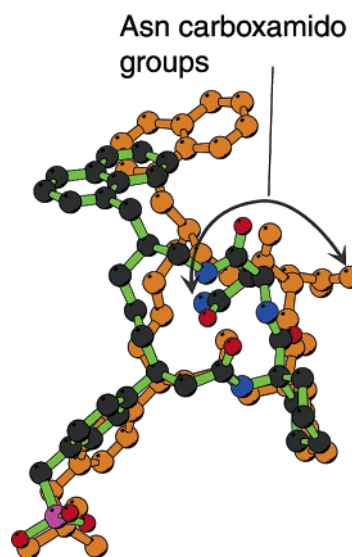


Figure 2. Overlay of energy-minimized conformations of **4** (colored by atom) and **12** (orange). The ligands were extracted from energy-minimized protein-ligand complexes.

observed in the synthesis of macrocycles **4** and **12**, where functionality at the pTyr mimetic α-position was absent, the inability of **18** to undergo ring closure potentially indicated that steric or electronic considerations presented by the α-amino functionality were incompatible with the olefin metathesis process.

Several factors were considered that might hinder olefin metathesis of **18**, including steric crowding between the highly hindered Ac₆C residue and the α-amino group of the pTyr-mimicking residue. Original reasons for using Ac₆C in the pTyr + 1 position of open-chain compounds such as **1** included its ability to induce bend conformations.¹³ Since in the context of macrocyclized ligands "bend conformations" are ensured without the aid of the Ac₆C residue, its importance as a bend inducer might be reduced in such compounds. Accordingly,

macrocycles were designed in which Ac₆c was replaced with residues containing less bulky groups. The synthesis of these compounds was first undertaken without functionality in the pTyr mimetic α -position. Ring-opened precursors **29**–**32** were prepared bearing α,α -substituents consisting of the following: H, H (Gly); H, *sec*-butyl (Ile); Me, Me (α -amino isobutyric acid); as well as the previously reported α,α -cyclohexane carboxylic acid.²⁰

Attempted olefin metathesis ring closure of precursors **29** and **30**, which bear a single substituent in this position, failed despite repeated attempts. Alternatively, ring closure of analogues containing two substituents (**31** and **32**) proceeded in good yield to provide macrocycles **35** and **36**. The synthesis of **36** was consistent with the previous synthesis of this compound.²⁰ These results indicated that successful ring-closing metathesis appeared to require an α,α -disubstituted residue proximal to the site of ring closure. It is known that such α,α -disubstituted residues induce bend structures,¹⁹ and our findings indicate that preexisting bend conformations favor olefin metathesis ring closure.

On the basis of the above study, fully elaborated macrocycles **45** and **6** bearing pTyr mimetic α -carboxymethyl substituents in addition to α,α -disubstituted residues at the pTyr mimetic + 1 position were prepared. Olefin metathesis ring closure leading to these analogues went smoothly in high yield. By comparison of ring-closing yields of **43** and **44** with **35** and **36**, it was observed that an approximate 20% increase in yield was obtained by introduction of a substituent at the pTyr mimetic α -position. The inability to induce ring closure of analogue **18**, which has an acetamido group at the pTyr mimetic α -position, indicated that the nature of the substituent at this position also affects ring closure. Finally, it was also observed that having a cyclohexyl-bearing Ac₆c residue at the pTyr mimetic + 1 position induced slightly more facile ring closure than the corresponding residue with α,α -dimethyl substituents. This further supported the importance of steric and conformational effects in ring-closing reactions.

Inhibition of Grb2 SH2 Domain Binding in Extracellular ELISA Assays. The current study was undertaken with the intent of preparing macrocycles that contain pTyr mimetic α -functionality. Additionally, since, for macrocycles such as **4**, the potential importance of a pTyr mimetic + 1 Ac₆c residue was uncertain because a ring structure is inherently constrained in bend conformations, we also examined various replacements for the Ac₆c residue. Although attempts to replace the Ac₆c residue in **4** with either a Gly (compound **33**) or an Ile residue (compound **34**) failed, ring closure of open-chain α,α -dimethyl-substituted analogues (**35** and **43**) was readily achieved. Final products **37** (IC₅₀ = 0.7 μ M) and **45** (IC₅₀ = 0.008 μ M), which were obtained following deprotection of **31** and **41**, respectively, showed reduced potency relative to their Ac₆c-containing counterparts **4** (IC₅₀ = 0.02 μ M¹⁷) and **6** (IC₅₀ = 0.002 μ M, Table 1), respectively. As with open-chain tripeptides in the original study by Novartis,¹³ this again shows the preference for an Ac₆c residue in the pTyr mimetic + 1 position. These results were supported by molecular modeling studies, which showed that compared with

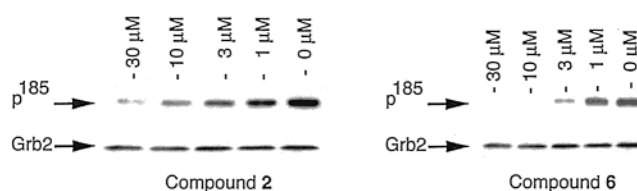


Figure 3. Association of Grb2 with p185^{erbB-2} in MDA-MB-453 cells following treatment with indicated concentrations of **2** and **6** measured by immunoprecipitation with Grb2 antibodies followed by Western blotting with pTyr antibodies as described in the Experimental Section.

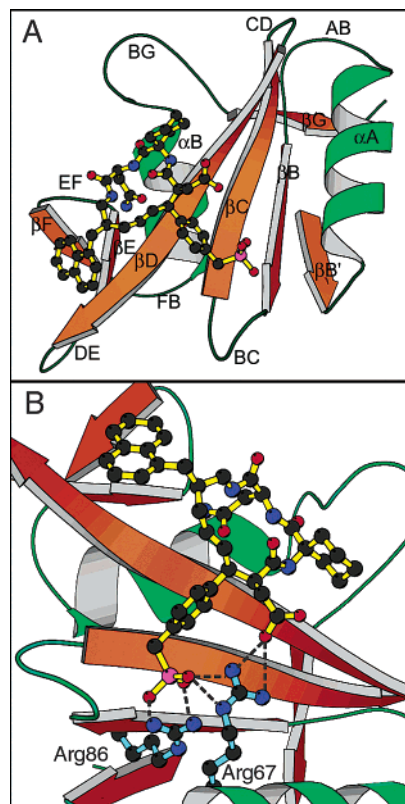


Figure 4. Molecular mechanics generated model of **6** (rendered in ball-and-stick fashion) complexed to the Grb2 SH2 domain as determined in the Experimental Section: (A) overall binding of **6** to the Grb2 SH2 domain; (B) highlight of ligand–protein interactions in the pTyr-binding pocket.

Ac₆c side chain C γ methylenes, α,α -dimethyl-substituted residues exhibit reduced van der Waals contacts with the protein pY + 1 binding sites (Phe β D5 and Gln β D3).

Intracellular Inhibition of Grb2 SH2 Domain Binding in Whole Cell Assays. The primary focus of the current study was introduction into macrocycles of carboxylic acid containing functionality at the pTyr mimetic α -position in order to enhance binding interactions with the Grb2 SH2 domain Arg67 residue. This objective was achieved with compound **6**, which exhibited high binding potency in an extracellular ELISA-based binding assay (Table 1). Of greater interest was the ability of **6** to function in whole-cell assays. The effective inhibition by synthetic ligands in whole-cell environments differs from extracellular ELISA assays in that ligands must cross cell membranes. Additionally, in cellular contexts, full-length Grb2 to which synthetic ligands must bind and cognate phosphorylated erbB-2 proteins with which the inhibitors must compete are much larger and more complex than in extracellular

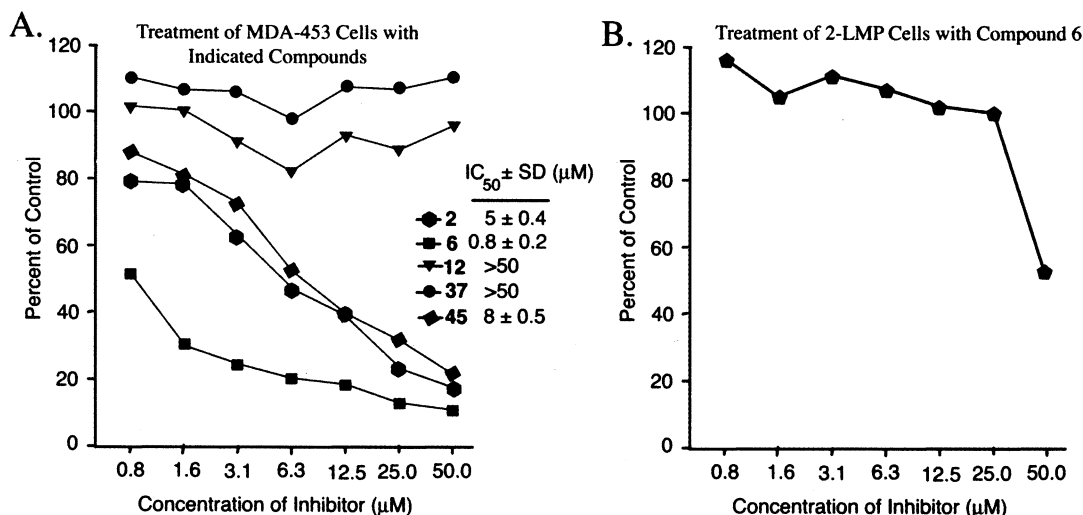


Figure 5. Plot of cell survival versus dose following treatment of MDA-MB-453 (A) and 2-LMP (B) cells in culture with varying concentrations of compounds as described in the Experimental Section.

ELISA assays (where competition is between the Grb2 SH2 domain fusion protein and a short pTyr-containing peptide). As shown in Figure 3, when open-chain OxoPmp (**2**) and functionalized macrocycle **6** were examined for their ability to inhibit the association of Grb2 with p185^{erbB-2}, **6** was significantly more potent than **2**. This is in contrast to macrocycle **4**, which had previously been shown to exhibit much reduced potency relative to **2** in a similar assay.¹⁷ Shown in Figure 4 (panel A) is the binding of **6** to the Grb2 SH2 domain as determined by molecular mechanics calculations, which highlights potential interactions of α -carboxymethyl functionality with the Arg67 residue (panel B). This represents another example where inclusion of the acidic functionality at the pTyr mimetic α -position enhances cellular Grb2 SH2 domain-binding potency.^{15,16}

Examination of Antiproliferative Effects in Breast Cancer Cell Cultures. Finally, it was of interest to examine the ability of macrocycles prepared in this study to inhibit the growth of breast cancer cells that are mitogenically driven through erbB-2 pathways. For these studies, MDA-MB-453/m1 cells (American Type Culture Collection, Rockville, MD) were treated with macrocycles **6**, **12**, **37**, **45** and with control open-chain **2** at varying concentrations for 8–10 days, and resulting cell numbers were then determined by direct counting. As shown in Figure 5A, similar to the previous report,¹⁷ OxoPmp (**2**) was able to exert a concentration-dependent antimitogenic effect, with an IC₅₀ value of approximately 5 μ M. In contrast, macrocycles **12** and **37**, which lack carboxylic acid containing functionality at the pTyr mimetic α -position, failed to exhibit antimitogenic effects up to 50 μ M concentrations. This was consistent with the previously reported poor antimitogenic profile of macrocycle **4**.¹⁷ Alternatively, macrocycles **6** and **45**, which possess carboxymethyl functionality at the pTyr mimetic α -position, did show good antimitogenic potencies, with Ac₆c-containing **6** exhibiting a submicromolar IC₅₀ value that was consistent with its ability to block the association of Grb2 to p185^{erbB-2} in the same cell line (Figure 3). When examined in the LMP-2 breast cancer cell line, which is not dependent on signaling through the erbB-2 system for growth and survival, macrocycle **6** had no effect at similar concen-

trations (Figure 5B), indicating that activity observed in MDA-MB-453 cells is most probably not associated with unrelated cytotoxicity.

Conclusions

The current study was predicated on previous findings that macrocyclization leading to compounds of type **4** could potentially enhance Grb2 SH2 domain-binding potency. Structural aspects of such macrocycles that might enhance Grb2 SH2 domain-binding potency and cellular efficacy were therefore examined. These included the role of ring size and the role of the pTyr mimetic + 1 residue in binding affinity. Here, it was found that enlarging the ring-closing bridge from three to four carbons significantly reduced binding potency and that the Ac₆c residue plays an important role in maintaining high inhibitory potency. However, the most significant aspect of the current study is its examination of the effects of carboxylic functionality at the pTyr mimetic α -position. It was observed that macrocycles such as **4**, **12**, and **37** that lack functionality at the pTyr mimetic α -position exhibit high Grb2 SH2 domain-binding potency in extracellular assays, yet they fail to demonstrate high potency in whole-cell assays. Alternatively, introduction of the carboxymethyl functionality at the pTyr mimetic α -position not only resulted in enhanced extracellular Grb2 SH2 domain-binding affinity but also conferred high potency in whole-cell systems. This latter fact may render such compounds as leads for the development of therapeutically relevant Grb2 SH2 domain signaling inhibitors.

Experimental Section

Cells and Cell Culture. Cell lines were obtained from the American Type Culture Collection (Rockville, MD) and Lombardi Cancer Center, Georgetown University Medical Center. Cells were routinely maintained in improved minimal essential medium (IMEM, Biofluids, Rockville, MD) with 10% fetal bovine serum. Cultures were maintained in a humidified incubator at 37 °C and 5% CO₂.

Inhibition of Grb2 SH2 Domain Binding Using ELISA Techniques. As previously reported,²⁸ a biotinylated phosphopeptide encompassing a Grb2 SH2 domain-binding sequence derived from SHC protein was bound at 20 ng/mL to 96-well

plates overnight. Nonspecific interactions were inhibited by 5% bovine serum albumin containing TBS. Samples of recombinant purified Grb2 SH2-GST fusion protein were preincubated with serial dilutions of inhibitors and then added into each well. After extensive washing with 0.1% bovine serum albumin in TBS, bound Grb2 SH2 domain was detected using anti-GST antibodies and goat antimouse antibody conjugated to alkaline phosphatase. Quantitation of bound alkaline phosphatase was achieved by a colorimetric reaction employing *p*-nitrophenyl phosphate as substrate. Each compound is subjected to a minimum of three determinations. Assays are conducted with a positive control of known potency, with additional controls being performed without peptide or protein.

Inhibition of Grb2 SH2 Domain Binding in Whole Cells. As previously reported,²⁸ erbB-2 overexpressing breast cancer cells, MDA-MB-453, were treated with inhibitors (25 μ M) for 3 h in serum-free IMEM medium (Gibco). Cells were washed twice with PBS to remove inhibitor, and then cell lysates were prepared using 1% Triton X-100 in PBS containing 0.2 mM NaVO₄. Grb2 and associated Grb2-binding proteins were immunoprecipitated from each lysate (500 μ g) with anti-Grb2 antibodies and collected using protein A Sepharose. Immunoprecipitated proteins were separated by SDS-PAGE on 8–16% gradient gels (Novex), and pTyr-containing proteins were detected by Western blotting using anti-phosphotyrosine antibodies (Upstate Biochemicals Inc.). Previous experiments have shown that a major tyrosine phosphorylated protein in these cells is the p185 erbB-2, which is overexpressed as a consequence of gene amplification. Western blotting with Grb2 MAb was done as a control. At least two determinations are performed for each compound.

Growth Inhibition of MDA-453 Breast Cancer Cells. Growth inhibition assays were run using 96-well plates. Individual wells were seeded with either MDA-453 cells (500 per well) or MDA-MB-231 (a subclone 2LMP; 2000 per well). Inhibitors were diluted to desired concentrations and added to plates, with fresh drug solutions being added every day for 5 days. Plates were incubated in a humidified incubator at 37 °C under 5% CO₂. Cell growth was detected using MTT (Sigma M-2128). Briefly, 20 μ L of MTT (0.5 mg/mL) was added to each well, followed by incubation under CO₂ (4 h). The medium was then removed, and cells dissolved were read at 570 nm using a microplate reader (Molecular Device). Final results were presented as a percent of control (no drug added).

Molecular Modeling. Molecular modeling of enzyme–substrate complexes was carried out using Sybyl 6.8 (Tripos, Inc., St. Louis, MO) on a Silicon Graphics Octane 2 workstation. Construction of the protein–ligand complex was based on the X-ray structure of the Grb2 SH2 domain complexed with a heptapeptide inhibitor (PDB entry 1TZE).¹² A model of the binding site was constructed consisting of residues between His 58 and Glu 152. Water molecules were removed, and backbone and side chain hydrogens were added using standard average bond angles and lengths. Amber4.1 atom type was given to the ligand, and Amber all-atom charges were applied to the protein and the ligand using the biopolymer module in Sybyl. Ligands were manually docked into the active site by adjusting torsion angles to those found in the X-ray structure. Protein–ligand complexes were minimized using a Powell conjugate gradient minimizer according to a MAXIMIN procedure with the Amber4.1 force field.

General Synthetic Methods. Elemental analyses were obtained from Atlantic Microlab Inc., Norcross, GA, and fast atom bombardment mass spectra (FAB-MS) were acquired with a VG Analytical 7070E mass spectrometer under the control of a VG 2035 data system. Where indicated, FAB-MS matrixes used were glycerol (Gly) or nitrobenzoic acid (NBA). ¹H NMR data were obtained on a Varian 400 MHz instrument and are reported in ppm relative to TMS and referenced to the solvent in which they were run. Solvent was removed by rotary evaporation under reduced pressure, and anhydrous solvents were obtained commercially and used without further drying. HPLC measurements were conducted using a Waters Prep LC4000 system having photodiode array detection and

binary solvent systems as indicated, where A = 0.1% aqueous TFA and B = 0.1% TFA in acetonitrile, and either Vydac C18 (10 μ m) Peptide & Protein or Advantage C18 (5 μ m) columns (preparative size, 20 mm diameter \times 250 mm long with a flow rate of 10 mL/min; semipreparative size, 10 mm diameter \times 250 mm long, with a flow rate of 2 mL/min).

General Procedure for Oxazolidinone Hydrolysis: Synthesis of Compounds 8, 15, and 39. To a solution of oxazolidinone **7**, **14**, or **38** (2.17 mmol) in THF/H₂O (3:1) (32 mL) at 0 °C was added H₂O₂ (30%, 1.107 mL, 10.85 mmol) via a syringe over 1 min. This was followed by the addition of LiOH (182.4 mg, 4.34 mmol) in H₂O (4.4 mL). After being stirred at 0 °C (1 h), the reaction mixture was raised to room temperature, and stirring was continued for an additional 6 h. A solution of Na₂SO₃ (1.37 g, 10.85 mmol) in H₂O (8.5 mL) was added to quench unreacted peroxide, and THF was evaporated at 30 °C. The resulting mixture was extracted with dichloromethane to remove cleaved oxazolidinone, and then the aqueous solution was acidified with ice-cooled 0.2 M aqueous HCl (54 mL), extracted with EtOAc, washed with brine, dried over Na₂SO₄, concentrated, and taken to dryness under high vacuum to provide free acids **8**, **15**, and **39**.

General Procedure for Fmoc Deprotection of Naphthyl-Containing Dipeptides: Synthesis of Compounds 9 and 25–27. To a solution of Fmoc-containing compounds **21–24** (1.0 mmol) in acetonitrile (5 mL) was added piperidine (1.0 mL), and the resulting solution was stirred at room temperature (2 h). Solvent was evaporated and residue was purified by silica gel chromatography to provide the corresponding free amines.

General Synthetic Procedure for Coupling of Amino Acid Analogues: Synthesis of Compounds 10, 16, 21–24, 29–32, and 40–42. To a solution of amine (0.626 mmol), amino acid (0.626 mmol), and HOBt or HOAt (0.626 mmol) in anhydrous DMF (5 mL) was added EDCI (0.688 mmol) at 0 °C, and the resulting mixture was stirred at room temperature (12–24 h). Then DMF was evaporated under high vacuum. Residue was dissolved in ethyl acetate (50 mL) and then washed sequentially with saturated aqueous NaHCO₃, H₂O, and brine and dried over Na₂SO₄. Concentration and purification by silica gel chromatography afforded the title compounds.

General Procedure for Ring-Closing Metathesis: Synthesis of Compounds 11, 35, 36, 43, and 44. To a solution of either **10**, **31**, **32**, **41**, or **42** (0.518 mmol) in anhydrous dichloromethane (150 mL) (deoxygenated by purging with argon) was added, via syringe, ruthenium catalyst (180 mg, 0.218 mmol) in dichloromethane (7 mL), and the solution was refluxed (60 °C) under argon with monitoring by TLC. Following reaction completion (approximate reaction times of 60 h were required), the solvent was evaporated and residue was purified by silica gel chromatography to provide the title compounds.

General Procedure for Removal of *tert*-Butyl Protection: Synthesis of Final Products 4, 6, 12, 37, and 45. The *tert*-butyl-protected analogues **11**, **35**, **36**, **43**, and **44** were treated with a solution of TFA/TES/H₂O (3.7 mL:0.1 mL:0.2 mL) (room temperature, 1 h), and then solvents were evaporated. To the residue was added ether, providing a precipitate, which was collected by centrifugation. The solid was washed with ether and separated again by centrifugation, and the resulting material was dried under high vacuum to provide the crude product, which was dissolved in acetonitrile/H₂O (1:1) (16 mL) and purified by reversed-phase HPLC to provide the desired products as white solids.

(4S)-3-[(3*R*)-3-(4-{[Bis(*tert*-butoxy)phosphono]methyl}phenyl)hex-5-enoyl]-4-phenyl-1,3-oxazolidin-2-one (7). Compound **7** was prepared as previously indicated.²¹

(3S)-3-(4-{[Bis(*tert*-butoxy)phosphono]methyl}phenyl)-hex-5-enoic acid (8). Mp 89–90 °C; ¹H NMR (CDCl₃) δ 7.15 (4H, m), 5.65 (1H, m), 4.97 (2H, m), 3.20 (1H, m), 2.93 (2H, d, *J* = 21.2 Hz), 2.72 (1H, dd, *J* = 6.4, 15.4 Hz), 2.57 (1H, dd, *J* = 8.8, 15.4 Hz), 2.38 (2H, t, *J* = 7.1 Hz), 1.39 (9H, s), 1.38 (9H, s); FAB-MS (–VE) *m/z* 395 (M – H)[–].

(3S)-N-[N-((1S)-1-{N-[(2S)-2-(Naphthylmethyl)pent-4-enyl]carbamoyl}-2-carbamoylethyl)carbamoyl]cyclohexyl-3-(4-{[bis(tert-butoxy)phosphono]methyl}phenyl)hex-5-enamide (10). Mp 82–83 °C; ¹H NMR (CDCl₃) δ 8.02 (1H, d, *J* = 8.5 Hz), 7.78 (2H, t, *J* = 7.9 Hz), 7.67 (1H, d, *J* = 2.4 Hz), 7.65 (1H, d, *J* = 2.8 Hz), 7.42 (2H, m), 7.31 (2H, m), 7.09 (1H, d, *J* = 2.5 Hz), 7.07 (1H, d, *J* = 2.5 Hz), 6.93 (1H, s), 6.90 (1H, s), 6.64 (1H, s), 6.01 (1H, s), 5.80 (1H, m), 5.45 (1H, m), 5.43 (1H, s), 5.03 (2H, m), 4.83 (2H, m), 4.63 (1H, m), 3.30 (1H, m), 3.09 (2H, m), 3.03 (1H, m), 2.98–2.84 (2H, m), 2.92 (2H, d, *J* = 21.4 Hz), 2.48 (2H, m), 2.39 (1H, dd, *J* = 4.8, 15.1 Hz), 2.20 (3H, m), 2.07 (2H, m), 1.95 (1H, d, *J* = 14.2 Hz), 1.82 (1H, d, *J* = 12.9 Hz), 1.69 (1H, dt, *J* = 3.6, 13.6 Hz), 1.60 (1H, dt, *J* = 3.2, 12.9 Hz), 1.46 (3H, m), 1.37 (9H, s), 1.35 (9H, s), 1.23 (1H, m), 1.09 (1H, m), 0.94 (1H, m); FAB-MS (+VE) *m/z* 843 (MH⁺).

2-[(9S,13S,18S)-8,11,21-Triaza-18-(4-{[bis(tert-butoxy)phosphono]methyl}phenyl)-13-(naphthylmethyl)-7,10,20-trioxospiro[5.15]henicos-15-en-9-yl]acetamide (11). Mp 215 °C; ¹H NMR (CDCl₃) δ 8.01 (1H, d, *J* = 8.2 Hz), 7.97 (1H, s), 7.78 (1H, dd, *J* = 1.3, 7.9 Hz), 7.64 (1H, d, *J* = 8.1 Hz), 7.54 (1H, s), 7.42 (2H, m), 7.29 (1H, dd, *J* = 7.0, 8.1 Hz), 7.22 (3H, m), 7.13 (1H, s), 7.11 (1H, s), 6.35 (1H, s), 6.23 (1H, s), 5.68 (1H, m), 5.53 (1H, s), 5.23 (1H, m), 4.77 (1H, s), 3.54 (1H, dd, *J* = 11.8, 22.7 Hz), 3.46 (1H, dd, *J* = 3.2, 13.6 Hz), 3.15 (1H, d, *J* = 13.2 Hz), 3.00 (1H, m), 2.97 (2H, d, *J* = 21.4 Hz), 2.86 (1H, d, *J* = 12.9 Hz), 2.62 (3H, m), 2.46–2.22 (4H, m), 1.88 (3H, m), 1.52 (5H, m), 1.36 (9H, s), 1.35 (9H, s), 1.29 (2H, m), 1.20 (2H, m); FAB-MS (+VE) *m/z* 815 (MH⁺).

2-[(9S,13S,18S)-8,11,21-Triaza-13-(naphthylmethyl)-7,10,20-trioxo-18-[4-(phosphonomethyl)phenyl]spiro[5.15]henicos-15-en-9-yl]acetamide (12). Mp 220 °C (dec); ¹H NMR (CD₃OD) δ 8.06 (1H, d, *J* = 8.1 Hz), 7.83 (1H, d, *J* = 7.9 Hz), 7.69 (1H, d, *J* = 6.0 Hz), 7.46 (2H, m), 7.34 (2H, m), 7.26 (2H, d, *J* = 7.2 Hz), 7.13 (2H, d, *J* = 7.5 Hz), 5.65 (1H, m), 5.21 (1H, m), 4.65 (1H, s), 3.51 (1H, m), 3.43 (1H, dd, *J* = 3.2, 13.5 Hz), 3.08 (2H, d, *J* = 21.2 Hz), 2.98 (1H, m), 2.90–2.50 (6H, m), 2.36 (1H, s), 2.25 (1H, d, *J* = 5.4 Hz), 2.08 (1H, m), 1.90 (1H, m), 1.75 (2H, m), 1.50 (5H, m), 1.33 (2H, m), 1.21 (2H, m); FAB-MS (–VE) *m/z* 701 (M – H)[–]. HR-FAB-MS calcd for C₃₈H₄₆N₄O₇P (M – H)[–]: 701.3104. Found: 701.314 43.

(4S)-3-[(2S,3R)-2-Azido-3-(4-{[bis(tert-butoxy)phosphono]methyl}phenyl)pent-4-enyl]-4-phenyl-1,3-oxazolidin-2-one (14). To a solution of sodium hexamethyldisilylamide (1.0 M in THF, 3.33 mL, 3.33 mmol) at –78 °C was added a precooled solution (–78 °C) of **13**²⁰ (1.596 g, 3.024 mmol) in THF (10 mL). The resulting solution quickly became deep-purple. After the mixture was stirred at –78 °C (30 min), a precooled (–78 °C) solution of trisyl azide (1.122 g, 3.628 mmol) was added, and the resulting solution was stirred at –78 °C (5 min). The reaction was quenched by the addition of glacial acetic acid (0.95 g, 16.6 mmol) followed by the addition of potassium acetate (1.217 g, 12.41 mmol), and the mixture was then stirred at 30 °C for an additional 1.5 h. To the mixture was added saturated aqueous NaHCO₃ solution (20 mL). Then THF was removed by evaporation, the residue was extracted with ethyl acetate, and the organic layers were washed with brine and dried over Na₂SO₄. Concentration and purification by silica gel chromatography (hexane/ethyl acetate, from 4:1 to 2:1) afforded **14** as an oil (1.26 g, 73% yield). ¹H NMR (CDCl₃) δ 7.40–7.14 (9H, m), 6.15 (1H, m), 5.48 (1H, d, *J* = 10.2 Hz), 5.29 (2H, dd, *J* = 10.2, 17.0 Hz), 4.90 (1H, dd, *J* = 2.8, 8.3 Hz), 4.24 (1H, t, *J* = 8.5 Hz), 4.04 (1H, dd, *J* = 2.7, 8.8 Hz), 3.82 (1H, t, *J* = 8.5 Hz), 3.01 (2H, d, *J* = 21.2 Hz), 1.46 (9H, s), 1.45 (9H, s); FAB-MS (+VE) *m/z* 569 (MH⁺).

(2S,3R)-2-Azido-3-(4-{[Bis(tert-butoxy)phosphono]methyl}phenyl)pent-4-enoic Acid (15). Mp 125 °C; ¹H NMR (CDCl₃) δ 7.22 (2H, d, *J* = 7.8 Hz), 7.14 (2H, dd, *J* = 2.4, 7.8 Hz), 6.16 (1H, m), 5.25 (2H, dd, *J* = 13.7, 16.6 Hz), 3.95 (1H, d, *J* = 9.3 Hz), 3.85 (1H, t, *J* = 9.3 Hz), 2.78 (2H, dd, *J* = 12.2, 21.2 Hz), 1.41 (9H, s), 1.35 (9H, s); FAB-MS (–VE) *m/z* 422 (M⁺ – H).

N-[N-((1S)-1-{N-[(2S)-2-(Naphthylmethyl)pent-4-enyl]carbamoyl}-2-carbamoylethyl)carbamoyl]cyclohexyl-(2S,3R)-2-azido-3-(4-{[bis(tert-butoxy)phosphono]methyl}phenyl)pent-4-enamide (16). Mp 148–149 °C; ¹H NMR (CDCl₃) δ 8.16 (1H, d, *J* = 7.8 Hz), 8.01 (1H, dd, *J* = 6.6, 14.8 Hz), 7.78 (1H, d, *J* = 8.2 Hz), 7.65 (2H, m), 7.44 (1H, dt, *J* = 1.4, 6.8 Hz), 7.38 (1H, dd, *J* = 1.2, 7.0 Hz), 7.33 (2H, m), 7.14 (2H, m), 7.04 (1H, s), 7.02 (1H, s), 6.97 (1H, s), 6.49 (1H, s), 6.10 (1H, m), 5.83 (1H, m), 5.10 (4H, m), 4.58 (1H, m), 4.17 (1H, d, *J* = 4.3 Hz), 3.93 (1H, dd, 4.1, 8.8 Hz), 3.23 (2H, dd, *J* = 5.6, 5.8 Hz), 3.02 (2H, m), 2.96 (2H, d, *J* = 21.4 Hz), 2.39 (1H, dd, *J* = 5.1, 15.0 Hz), 2.10 (3H, m), 1.84 (2H, m), 1.74 (1H, m), 1.59 (3H, m), 1.39 (9H, s), 1.37 (9H, s), 1.23 (4H, m), 0.80 (1H, m); FAB-MS (+VE) *m/z* 870 (MH⁺).

N-[N-((1S)-1-{N-[(2S)-2-(Naphthylmethyl)pent-4-enyl]carbamoyl}-2-carbamoylethyl)carbamoyl]cyclohexyl-(2S,3R)-2-amino-3-(4-{[bis(tert-butoxy)phosphono]methyl}phenyl)pent-4-enamide (17). To a solution of **16** (363 mg, 0.418 mmol) in a mixture of THF/H₂O (8 mL:0.5 mL) was added triphenylphosphine (163 mg, 0.618 mmol, 1.5 equiv), and the resulting mixture was refluxed (12 h). Then THF was removed by evaporation. The resulting aqueous solution was extracted with ethyl acetate, and the organic layers were washed with brine and dried over Na₂SO₄. After removal of solvent, residue was purified by silica gel chromatography (CHCl₃/methanol, from 100:0 to 9:1) to provide **17** as a sticky oil (341 mg; 97% yield). ¹H NMR (CDCl₃) δ 8.12 (1H, m), 7.98 (2H, m), 7.77 (1H, d, *J* = 7.8 Hz), 7.64 (1H, dd, *J* = 4.7, 5.1 Hz), 7.43 (1H, dt, *J* = 1.2, 6.6 Hz), 7.36 (1H, m), 7.32 (2H, m), 7.12 (2H, m), 7.02 (1H, s), 7.00 (1H, s), 6.68 (1H, s), 5.98 (1H, m), 5.79 (1H, m), 5.31 (1H, s), 5.08 (4H, m), 4.58 (1H, m), 3.87 (1H, m), 3.60 (1H, d, *J* = 4.3 Hz), 3.21 (2H, t, *J* = 5.5 Hz), 3.07 (1H, m), 2.97 (1H, m), 2.95 (2H, d, *J* = 21.4 Hz), 2.38 (1H, dd, *J* = 5.1, 14.8 Hz), 2.09 (3H, m), 1.87 (2H, m), 1.74 (1H, m), 1.57 (3H, m), 1.38 (9H, s), 1.37 (9H, s), 1.23 (4H, m), 0.77 (1H, m); FAB-MS (+VE) *m/z* 844 (MH⁺).

N-[N-((1S)-1-{N-[(2S)-2-(Naphthylmethyl)pent-4-enyl]carbamoyl}-2-carbamoylethyl)carbamoyl]cyclohexyl-(2S,3R)-2-(acetyl-amino)-3-(4-{[bis(tert-butoxy)phosphono]methyl}phenyl)pent-4-enamide (18). To a solution of **17** (84 mg, 0.1 mmol) in anhydrous dichloromethane (10 mL) was added acetic anhydride (189 μL, 2.0 mmol, 20 equiv) and triethylamine (355 μL, 2.4 mmol, 24 equiv), and the resulting mixture was stirred at room temperature (12 h). The reaction was quenched by addition of aqueous NaHCO₃, and the solution was extracted with dichloromethane and washed with brine and dried over Na₂SO₄. Solvent was removed by evaporation, and residue was purified by silica gel chromatography (CHCl₃/methanol, 9:1) to provide **18** as a foam (71 mg, 80% yield). ¹H NMR (CDCl₃) δ 8.02 (1H, d, *J* = 8.2 Hz), 7.80 (1H, d, *J* = 7.8 Hz), 7.68 (1H, d, *J* = 7.4 Hz), 7.46 (3H, m), 7.34 (3H, m), 7.12 (2H, m), 7.02 (2H, m), 6.75 (1H, s), 6.67 (1H, s), 6.11 (1H, s), 5.80 (3H, m), 5.00 (4H, m), 4.64 (2H, m), 3.57 (1H, m), 3.35 (1H, m), 3.11 (1H, m), 3.04 (1H, m), 2.98 (1H, m), 2.93 (2H, d, *J* = 21.4 Hz), 2.74 (1H, m), 2.60 (1H, m), 2.10 (3H, m), 1.83 (3H, s), 1.80 (2H, m), 1.63 (2H, m), 1.40 (9H, s), 1.37 (9H, s), 1.28 (2H, m), 1.09 (2H, m), 0.81 (1H, m), 0.74 (1H, m); FAB-MS (+VE) *m/z* 886 (MH⁺).

(2S)-N-[(2S)-2-(Naphthylmethyl)pent-4-enyl]-2-(2-aminoacetyl-amino)-3-carbamoylpropanamide (25). Mp 182 °C; ¹H NMR (CD₃OD) δ 7.98 (1H, d, *J* = 8.6 Hz), 7.78 (1H, d, *J* = 8.8 Hz), 7.66 (1H, d, *J* = 7.8 Hz), 7.46 (1H, m), 7.39 (1H, m), 7.29 (2H, m), 5.80 (1H, m), 5.01 (2H, m), 4.68 (1H, dd, *J* = 6.1, 6.6 Hz), 3.25 (2H, m), 3.05 (2H, m), 2.97 (2H, m), 2.63 (2H, d, *J* = 6.3 Hz), 2.06 (3H, m); FAB-MS (+VE) *m/z* 397 (MH⁺).

N-[(1S)-1-{N-[(2S)-2-(Naphthylmethyl)pent-4-enyl]carbamoyl}-2-carbamoylethyl)-(2S,3R)-2-amino-3-methylpentanamide (26). Mp 152–153 °C; ¹H NMR (CD₃OD) δ 7.98 (1H, d, *J* = 8.0 Hz), 7.80 (1H, d, *J* = 8.4 Hz), 7.68 (1H, d, *J* = 7.8 Hz), 7.48 (1H, m), 7.40 (1H, m), 7.31 (2H, m), 5.80 (1H, m), 5.02 (2H, m), 4.67 (1H, dd, *J* = 6.4, 6.6 Hz), 3.25 (2H, m), 3.13 (2H, m), 2.98 (2H, m), 2.63 (2H, d, *J* = 6.4 Hz), 2.07 (2H,

m), 1.66 (1H, m), 1.40 (1H, m), 1.08 (1H, m), 0.87 (3H, d, $J = 6.8$ Hz), 0.81 (3H, t, $J = 7.4$ Hz); FAB-MS (+VE) m/z 453 (MH⁺).

***N*-(1*S*)-1-[*N*-(2*S*)-2-(Naphthylmethyl)pent-4-enyl]carbamoyl-2-carbamoylethyl-2-amino-2-methylpropanamide (27)**. Mp 89 °C; ¹H NMR (CDCl₃) δ 8.80 (1H, d, $J = 7.0$ Hz), 7.98 (1H, d, $J = 8.2$ Hz), 7.85 (1H, m), 7.72 (1H, d, $J = 8.2$ Hz), 7.49 (2H, m), 7.38 (1H, m), 7.31 (1H, d, $J = 7.0$ Hz), 7.21 (1H, m), 6.29 (1H, s), 5.81 (1H, m), 5.54 (1H, s), 5.09 (2H, m), 4.61 (1H, m), 3.25 (2H, m), 3.06 (1H, dd, $J = 6.6, 14.0$ Hz), 2.96 (1H, dd, $J = 6.6, 14.0$ Hz), 2.80 (1H, dd, $J = 4.3, 15.2$ Hz), 2.54 (1H, dd, $J = 7.0, 15.2$ Hz), 2.11 (3H, d, $J = 6.2$ Hz), 1.36 (3H, s), 1.34 (3H, s); FAB-MS (+VE) m/z 425 (MH⁺).

(2*S*)-*N*-(2*S*)-2-(Naphthylmethyl)pent-4-enyl-2-[(aminocyclohexyl)carbonylamino]-3-carbamoylpropanamide (9). ¹H NMR (CDCl₃): δ 8.89 (1H, d, $J = 6.8$ Hz), 7.98 (1H, m), 7.85 (1H, m), 7.72 (1H, d, $J = 7.8$ Hz), 7.55–7.26 (7H, m), 6.31 (1H, s, br), 5.91–5.75 (1H, m), 5.54 (1H, s, br), 5.13–5.07 (2H, m), 4.68 (1H, dd, $J = 6.1, 10.7$ Hz), 3.35–3.21 (2H, m), 3.08 (1H, dd, $J = 6.6, 14.2$ Hz), 2.97 (1H, dd, $J = 6.4, 13.9$ Hz), 2.83 (1H, dd, $J = 4.4, 15.1$ Hz), 2.56 (1H, dd, $J = 6.5, 14.6$ Hz), 2.17 (2H, d, $J = 5.9$ Hz), 2.05–1.23 (11H, m). FAB-MS (+VE) m/z 465 (MH⁺).

(3*R*)-*N*-[*N*-(1*S*)-1-[*N*-(2*S*)-2-(Naphthylmethyl)pent-4-enyl]carbamoyl]-2-carbamoylethylcarbamoyl[methyl]-3-(4-{[bis(*tert*-butoxy)phosphono]methyl}phenyl)pent-4-enamide (29). Mp 120 °C; ¹H NMR (CDCl₃) δ 7.95 (1H, d, $J = 8.4$ Hz), 7.78 (1H, dd, $J = 1.3, 8.1$ Hz), 7.66 (1H, d, $J = 7.9$ Hz), 7.61 (1H, d, $J = 7.9$ Hz), 7.43 (2H, m), 7.29 (2H, m), 7.12 (1H, d, $J = 2.4$ Hz), 7.09 (1H, d, $J = 2.4$ Hz), 7.01 (1H, s), 6.98 (1H, s), 6.90 (1H, m), 6.78 (1H, s), 5.81 (2H, m), 5.71 (1H, s), 5.03 (2H, m), 4.93 (2H, m), 4.68 (1H, dd, $J = 7.1, 12.4$ Hz), 3.75 (1H, m), 3.65 (2H, m), 3.28 (1H, m), 3.07 (1H, m), 2.97 (2H, m), 2.93 (2H, d, $J = 21.4$ Hz), 2.70 (1H, dd, $J = 4.9, 15.9$ Hz), 2.52 (3H, m), 2.06 (3H, m), 1.37 (9H, s), 1.35 (9H, s); FAB-MS (+VE) m/z 761 (MH⁺).

(3*R*)-*N*-[*N*-(1*S*)-1-[*N*-(2*S*)-2-(Naphthylmethyl)pent-4-enyl]carbamoyl]-2-carbamoylethylcarbamoyl-(1*S*,2*R*)-2-methylbutyl-3-(4-{[bis(*tert*-butoxy)phosphono]methyl}phenyl)pent-4-enamide (30). Mp 175–176 °C; ¹H NMR (CD₃OD) δ 7.98 (1H, d, $J = 8.2$ Hz), 7.79 (1H, dd, $J = 1.2, 8.6$ Hz), 7.65 (1H, dd, $J = 2.3, 7.4$ Hz), 7.43 (1H, m), 7.38 (1H, m), 7.29 (2H, m), 7.10 (1H, d, $J = 2.3$ Hz), 7.08 (1H, d, $J = 2.3$ Hz), 7.00 (1H, s), 6.97 (1H, s), 5.82 (2H, m), 5.00 (2H, m), 4.89 (2H, m), 4.55 (1H, t, $J = 6.2$ Hz), 3.98 (1H, d, $J = 7.0$ Hz), 3.66 (1H, dd, $J = 7.4, 15.6$ Hz), 3.19 (1H, dd, $J = 6.6, 13.6$ Hz), 3.02 (1H, m), 2.97 (1H, m), 2.95 (2H, d, $J = 21.4$ Hz), 2.63 (3H, m), 2.50 (1H, dd, $J = 6.2, 14.0$ Hz), 2.10 (2H, m), 1.99 (1H, m), 1.74 (1H, m), 1.42 (1H, m), 1.38 (9H, s), 1.34 (9H, s), 1.13 (1H, m), 0.81 (6H, m), 0.69 (1H, m); FAB-MS (+VE) m/z 817 (MH⁺).

(3*R*)-*N*-[*N*-(1*S*)-1-[*N*-(2*S*)-2-(Naphthylmethyl)pent-4-enyl]carbamoyl]-2-carbamoylethylcarbamoyl[isopropyl]-3-(4-{[bis(*tert*-butoxy)phosphono]methyl}phenyl)pent-4-enamide (31). Mp 108–110 °C; ¹H NMR (CDCl₃) δ 8.04 (1H, d, $J = 8.2$ Hz), 7.80 (2H, m), 7.69 (2H, m), 7.44 (2H, m), 7.34 (2H, m), 7.13 (1H, d, $J = 2.7$ Hz), 7.11 (1H, d, $J = 2.7$ Hz), 6.96 (1H, s), 6.94 (1H, s), 6.79 (1H, s), 6.51 (1H, s), 5.84 (2H, m), 5.58 (1H, s), 5.05 (2H, m), 4.95 (2H, m), 4.62 (1H, m), 3.71 (1H, dd, $J = 7.0, 14.0$ Hz), 3.32 (1H, m), 3.10 (2H, m), 3.00 (1H, m), 2.96 (2H, d, $J = 21.4$ Hz), 2.90 (1H, m), 2.54 (2H, m), 2.45 (1H, dd, $J = 5.1, 15.2$ Hz), 2.23 (1H, m), 2.10 (2H, m), 1.41 (9H, s), 1.39 (9H, s), 1.36 (3H, s), 1.32 (3H, s); FAB-MS (+VE) m/z 789 (MH⁺).

(3*R*)-*N*-[*N*-(1*S*)-1-[*N*-(2*S*)-2-(Naphthylmethyl)pent-4-enyl]carbamoyl]-2-carbamoylethylcarbamoyl[cyclohexyl]-3-(4-{[bis(*tert*-butoxy)phosphono]methyl}phenyl)pent-4-enamide (32). Mp 87–88 °C; ¹H NMR (CDCl₃) δ 8.05 (1H, d, $J = 8.1$ Hz), 7.85–7.64 (4H, m), 7.55–7.38 (4H, m), 7.15 (2H, dd, $J = 2.4, 7.8$ Hz), 6.99 (2H, d, $J = 8.1$ Hz), 6.28 (1H, s, br), 5.96–5.77 (3H, m), 5.41 (1H, s, br), 5.13–4.90 (4H, m), 4.72 (1H, m), 3.73 (1H, m), 3.37 (1H, m), 3.22–2.91 (6H, m), 2.65–2.45 (2H, m), 2.30–2.01 (3H, m), 1.95–1.09 (11H, m), 1.43 (9H, s), 1.41 (9H, s); FAB-MS (+VE) m/z 828 (MH⁺).

2-[(1*S*,5*S*,9*R*)-3,12,15-Triaza-9-(4-{[bis(*tert*-butoxy)phosphono]methyl}phenyl)-13,13-dimethyl-5-(naphthylmethyl)-2,11,14-trioxocyclopentadec-7-enyl]acetamide (35). Mp 218 °C; ¹H NMR (CD₃OD) δ 8.78 (1H, s), 8.48 (1H, d, $J = 8.2$ Hz), 8.14 (1H, d, $J = 8.5$ Hz), 7.78 (1H, dd, $J = 1.2, 8.2$ Hz), 7.74 (1H, m), 7.65 (1H, d, $J = 7.6$ Hz), 7.48 (1H, m), 7.40 (1H, m), 7.30 (2H, m), 7.12 (2H, m), 5.61 (1H, m), 5.39 (1H, m), 4.50 (1H, m), 3.82 (1H, m), 3.72 (1H, dd, $J = 6.6, 13.0$ Hz), 3.28 (1H, m), 2.98 (1H, m), 2.96 (2H, d, $J = 21.4$ Hz), 2.78 (1H, m), 2.63 (2H, m), 2.46 (2H, m), 2.20 (1H, m), 1.98 (1H, m), 1.80 (1H, m), 1.45 (3H, s), 1.37 (3H, s), 1.35 (18H, s); FAB-MS (+VE) m/z 761 (MH⁺).

2-[(9*S*,13*S*,17*R*)-8,11,20-Triaza-17-(4-{[bis(*tert*-butoxy)phosphono]methyl}phenyl)-13-(naphthylmethyl)-7,10,19-trioxospiro[5.14]icos-15-en-9-yl]acetamide (36). Mp 210 °C; ¹H NMR (CDCl₃) δ 8.30–8.00 (2H, m), 7.83 (1H, m), 7.69 (1H, d, $J = 7.8$ Hz), 7.59 (1H, m), 7.55–7.30 (4H, m), 7.25–7.05 (4H, m), 6.35 (1H, s, br), 6.28 (1H, s, br), 5.66 (1H, dd, $J = 9.3, 14.4$ Hz), 5.31 (1H, m), 5.08 (1H, s, br), 4.66 (1H, m), 3.90–3.70 (2H, m), 3.62 (1H, m), 3.33–3.08 (2H, m), 3.06–2.88 (4H, m), 2.85–2.50 (4H, m), 2.37–1.15 (11H, m), 1.42 (18H, s); FAB-MS (+VE) m/z 801 (MH⁺).

2-[(1*S*,5*S*,9*R*)-3,12,15-Triaza-13,13-dimethyl-5-(naphthylmethyl)-2,11,14-trioxo-9-[4-(phosphonomethyl)phenyl]cyclopentadec-7-enyl]acetamide (37). Mp 230 °C (dec); ¹H NMR (CD₃OD) δ 8.79 (1H, s), 8.48 (1H, d, $J = 8.0$ Hz), 8.14 (1H, d, $J = 8.4$ Hz), 7.78 (1H, d, $J = 7.8$ Hz), 7.74 (1H, m), 7.64 (1H, d, $J = 7.4$ Hz), 7.48 (1H, t, $J = 7.0$ Hz), 7.40 (1H, t, $J = 7.4$ Hz), 7.28 (2H, m), 7.14 (4H, m), 5.60 (1H, m), 5.37 (1H, m), 4.50 (1H, m), 3.80 (1H, dd, $J = 10.1, 10.7$ Hz), 3.72 (1H, dd, $J = 6.3, 13.7$ Hz), 3.31 (1H, m), 3.02 (2H, d, $J = 21.3$ Hz), 2.97 (1H, m), 2.78 (1H, m), 2.65 (1H, dd, $J = 10.1, 13.5$ Hz), 2.58 (1H, dd, $J = 2.3, 12.5$ Hz), 2.49 (1H, dd, $J = 4.7, 15.2$ Hz), 2.42 (1H, dd, $J = 12.3, 12.5$ Hz), 2.19 (1H, m), 1.95 (1H, m), 1.78 (1H, m), 1.46 (3H, s), 1.36 (3H, s); FAB-MS (–VE) m/z 647 (MH⁺). HR-FAB-MS calcd for C₃₄H₄₀N₄O₇P (M – H)[–]: 647.2635. Found: 647.2667.

2-[(9*S*,13*S*,17*R*)-8,11,20-Triaza-13-(naphthylmethyl)-7,10,19-trioxo-17-[4-(phosphonomethyl)phenyl]spiro[5.14]icos-15-en-9-yl]acetamide (4). Mp 225 °C (dec); ¹H NMR (400 MHz, d₆-DMSO) δ 8.40 (1H, s), 8.23 (1H, d, $J = 7.8$ Hz), 8.12 (1H, d, $J = 8.1$ Hz), 7.89 (1H, d, $J = 7.6$ Hz), 7.75 (1H, m), 7.56–7.38 (6H, m), 7.15–7.02 (5H, m), 5.55 (1H, dd, $J = 9.5, 14.2$ Hz), 5.37 (1H, m), 4.27 (1H, m), 3.86 (1H, m), 3.59 (1H, dd, $J = 5.6, 11.7$ Hz), 3.16 (1H, dd, $J = 5.7, 14.4$ Hz), 2.95–2.30 (8H, m), 2.25–1.10 (13H, m); FAB-MS (–VE) m/z 687.6 (M – H)[–]. HR-FAB-MS calcd for C₃₇H₄₄N₄O₇P (M – H)[–]: 687.2948. Found: 687.2958.

***tert*-Butyl 3-[(4*S*)-2-Oxo-4-phenyl(1,3-oxazolidin-3-yl)-carbonyl]-(3*S*,4*S*)-4-(4-{[bis(*tert*-butoxy)phosphono]methyl}phenyl)hex-5-enoate (38)**. To a solution of sodium hexamethyldisilylamide (1.0 M in THF, 1.2 mL, 1.2 mmol) at –78 °C was added a solution of **13** (527 mg, 1.0 mmol) in THF (2 mL). The solution quickly became deep-purple. After the mixture was stirred at –78 °C (30 min), a precooled (–78 °C) solution of *tert*-butyl bromoacetate (234 mg, 1.2 mmol) was added, and the resulting solution was stirred at –78 °C (2 h). Then the mixture was brought to room temperature and stirred overnight. The reaction was quenched by addition of saturated aqueous NH₄Cl (20 mL), and then THF was evaporated and the resulting liquid was extracted with ethyl acetate, washed with brine, and dried over Na₂SO₄. Concentration and purification by silica gel chromatography (hexanes/ethyl acetate, 1:1.25) afforded **38** as an oil (495 mg, 77% yield). ¹H NMR (CDCl₃) δ 7.30–7.15 (9H, m), 6.08 (1H, m), 5.18 (2H, m), 4.80 (2H, m), 4.04 (1H, dd, $J = 8.1, 8.6$ Hz), 3.95 (1H, dd, $J = 2.4, 8.6$ Hz), 3.35 (1H, t, $J = 9.8$ Hz), 3.02 (2H, d, $J = 21.5$ Hz), 2.77 (1H, dd, $J = 11.0, 17.1$ Hz), 2.61 (1H, dd, $J = 3.9, 17.1$ Hz), 1.49 (18H, s), 1.31 (9H, s); FAB-MS (+VE) m/z 642 (MH⁺).

(2*S*,3*S*)-3-(4-{[Bis(*tert*-butoxy)phosphono]methyl}phenyl)-2-[(*tert*-butyl)oxycarbonyl]methyl]pent-4-enoic Acid (39). Mp 155 °C; ¹H NMR (CDCl₃) δ 7.16 (4H, m), 5.97 (1H, m), 5.15 (2H, m), 3.50 (1H, t, $J = 9.3$ Hz), 3.15 (1H,

dt, $J = 4.4, 9.8$ Hz), 2.83 (2H, dd, $J = 3.4, 21.5$ Hz), 2.60 (2H, m), 1.43 (9H, s), 1.41 (9H, s), 1.37 (9H, s); FAB-MS (–VE) m/z 495 (M – H)[–].

tert-Butyl 3-(N-{[N-((1S)-1-[N-((2S)-2-(Naphthylmethyl)pent-4-enyl]carbamoyl)-2-carbamoylethyl]carbamoyl]methyl}carbamoyl)-(3S,4S)-4-(4-{[bis(tert-butoxy)phosphono]methyl}phenyl)hex-5-enoate (40). Mp 104–105 °C; ¹H NMR (CDCl₃): δ 7.97 (1H, d, $J = 8.5$ Hz), 7.80 (1H, dd, $J = 1.4, 8.2$ Hz), 7.68 (1H, d, $J = 7.9$ Hz), 7.45 (2H, m), 7.34 (3H, m), 7.12 (3H, m), 7.05 (1H, s), 7.03 (1H, s), 6.40 (1H, s), 5.79 (2H, m), 5.60 (1H, s), 5.04 (4H, m), 4.61 (1H, dd, $J = 6.4, 13.0$ Hz), 3.59 (1H, dd, $J = 5.4, 16.7$ Hz), 3.33 (3H, m), 3.13 (1H, m), 3.00 (2H, d, $J = 6.7$ Hz), 2.92 (2H, d, $J = 21.5$ Hz), 2.86 (1H, dt, $J = 3.7, 10.1$ Hz), 2.70 (2H, m), 2.58 (1H, m), 2.49 (1H, dd, $J = 3.8, 17.1$ Hz), 2.12 (3H, m), 1.37 (9H, s), 1.35 (9H, s), 1.34 (9H, s); FAB-MS (+VE) m/z 875 (MH⁺).

tert-Butyl 3-(N-{1-[N-((1S)-1-[N-((2S)-2-(Naphthylmethyl)pent-4-enyl]carbamoyl)-2-carbamoylethyl]carbamoyl]isopropyl}carbamoyl)-(3S,4S)-4-(4-{[bis(tert-butoxy)phosphono]methyl}phenyl)hex-5-enoate (41). Mp 92 °C; ¹H NMR (CDCl₃): δ 8.04 (1H, d, $J = 8.5$ Hz), 7.80 (1H, dd, $J = 1.3, 8.5$ Hz), 7.68 (1H, m), 7.48 (1H, m), 7.42 (1H, m), 7.35 (3H, m), 7.10 (2H, m), 7.00 (1H, m), 6.91 (1H, s), 6.89 (1H, s), 6.63 (1H, s), 6.00 (1H, m), 5.84 (1H, m), 5.66 (1H, m), 5.38 (1H, s), 5.05 (2H, m), 4.92 (2H, m), 4.45 (1H, dd, $J = 6.2, 13.0$ Hz), 3.29 (1H, m), 3.11 (2H, m), 3.04 (2H, m), 2.92 (2H, d, $J = 21.4$ Hz), 2.78 (2H, m), 2.66 (1H, dd, $J = 7.5, 15.2$ Hz), 2.48 (2H, d, $J = 7.0$ Hz), 2.16 (2H, m), 2.06 (1H, m), 1.39 (9H, s), 1.37 (9H, s), 1.35 (9H, s), 1.14 (3H, s), 1.04 (3H, s); FAB-MS (+VE) m/z 903 (MH⁺).

tert-Butyl 3-(N-{[N-((1S)-1-[N-((2S)-2-(Naphthylmethyl)pent-4-enyl]carbamoyl)-2-carbamoylethyl]carbamoyl]cyclohexyl}carbamoyl)-(3S,4S)-4-(4-{[bis(tert-butoxy)phosphono]methyl}phenyl)hex-5-enoate (42). Mp 85 °C; ¹H NMR (CDCl₃): δ 8.05 (1H, d, $J = 8.4$ Hz), 7.81 (1H, d, $J = 8.5$ Hz), 7.68 (1H, dd, $J = 2.6, 6.6$ Hz), 7.45 (2H, m), 7.36 (3H, m), 7.09 (2H, m), 6.90 (1H, s), 6.88 (1H, s), 6.74 (1H, s), 6.06 (1H, s), 5.84 (1H, m), 5.61 (1H, m), 5.38 (1H, s), 5.07 (2H, m), 4.90 (2H, m), 4.57 (1H, dd, $J = 7.4, 12.5$ Hz), 3.32 (1H, m), 3.20 (1H, dd, $J = 10.0, 10.4$ Hz), 3.04 (2H, m), 2.93 (4H, m), 2.74 (1H, m), 2.62 (1H, m), 2.46 (2H, m), 2.18 (2H, m), 2.08 (1H, m), 1.70 (6H, m), 1.40 (9H, s), 1.38 (9H, s), 1.36 (9H, s), 1.05 (3H, m), 0.78 (1H, m); FAB-MS (+VE) m/z 943 (MH⁺).

tert-Butyl 2-[(1S,7S,11S,15S)-3,6,9-Triaza-15-(4-{[bis(tert-butoxy)phosphono]methyl}phenyl)-7-(carbamoylmethyl)-4,4-dimethyl-11-(naphthylmethyl)-2,5,8-trioxo-cyclopentadec-13-enyl]acetate (43). Mp 229–230 °C; ¹H NMR (CD₃OD) δ 8.88 (1H, s), 8.50 (1H, d, $J = 8.5$ Hz), 8.18 (1H, d, $J = 8.5$ Hz), 7.78 (1H, dd, $J = 1.2, 8.2$ Hz), 7.66 (2H, m), 7.48 (1H, m), 7.40 (1H, m), 7.32 (2H, m), 7.18 (3H, m), 5.84 (1H, ddd, $J = 2.0, 10.4, 12.3$ Hz), 5.45 (1H, ddd, $J = 3.1, 10.5, 14.2$ Hz), 4.53 (1H, m), 3.98 (1H, d, $J = 10.3$ Hz), 3.72 (1H, dd, $J = 6.9, 13.2$ Hz), 3.34 (1H, dd, $J = 4.4, 13.3$ Hz), 3.05 (1H, dt, $J = 12.4, 2.3$ Hz), 3.00 (2H, d, $J = 21.4$ Hz), 2.98 (1H, m), 2.80 (2H, m), 2.67 (1H, dd, $J = 10.2, 13.6$ Hz), 2.47 (1H, dd, $J = 4.8, 15.2$ Hz), 2.22 (1H, m), 2.03 (2H, m), 1.94 (1H, m), 1.418 (3H, s), 1.412 (3H, s), 1.352 (9H, s), 1.348 (9H, s), 1.32 (9H, s).

tert-Butyl 2-[(9S,10S,14S,18S)-7,16,19-Triaza-10-(4-{[bis(tert-butoxy)phosphono]methyl}phenyl)-18-(carbamoylmethyl)-14-(naphthylmethyl)-8,17,20-trioxospiro[5.14]icos-11-en-9-yl]acetate (44). Mp 221 °C; ¹H NMR (CDCl₃): δ 8.12 (1H, d, $J = 8.5$ Hz), 8.04 (1H, d, $J = 7.9$ Hz), 7.74 (1H, d, $J = 8.4$ Hz), 7.64 (1H, d, $J = 7.9$ Hz), 7.49 (1H, m), 7.44 (1H, m), 7.34 (2H, m), 7.25 (1H, m), 7.14 (4H, m), 6.36 (1H, s), 6.05 (1H, s), 5.74 (1H, dd, $J = 10.1, 14.1$ Hz), 5.26 (1H, m), 4.98 (1H, s), 4.63 (1H, m), 3.92 (1H, d, $J = 9.4$ Hz), 3.74 (1H, dd, $J = 6.1, 13.8$ Hz), 3.27 (1H, dd, $J = 5.0, 13.8$ Hz), 3.09 (1H, m), 3.00 (1H, m), 2.95 (2H, d, $J = 21.4$ Hz), 2.81 (1H, dd, $J = 11.8, 17.3$ Hz), 2.72 (1H, m), 2.64 (1H, dd, $J = 9.7, 13.8$ Hz), 2.25 (2H, m), 2.10 (3H, m), 1.88 (1H, m),

1.70 (6H, m), 1.52 (3H, m), 1.35 (9H, s), 1.34 (9H, s), 1.30 (9H, s); FAB-MS (+VE) m/z 915 (MH⁺).

2-[(1S,7S,11S,15S)-3,6,9-Triaza-7-(carbamoylmethyl)-4,4-dimethyl-11-(naphthylmethyl)-2,5,8-trioxo-15-[4-(phosphonomethyl)phenyl]cyclopentadec-13-enyl]acetic Acid (45). Mp 240 °C (dec); ¹H NMR (CD₃OD) δ 8.86 (1H, s), 8.48 (1H, d, 8.2 Hz), 8.18 (1H, d, $J = 8.6$ Hz), 7.78 (1H, d, $J = 7.6$ Hz), 7.68 (2H, m), 7.48 (1H, dd, $J = 6.8, 7.4$ Hz), 7.40 (1H, t, $J = 7.6$ Hz), 7.32 (2H, m), 7.20 (3H, s), 5.85 (1H, m), 5.44 (1H, m), 4.53 (1H, m), 3.97 (1H, d, $J = 9.4$ Hz), 3.72 (1H, dd, $J = 7.2, 13.3$ Hz), 3.34 (1H, m), 3.10 (1H, m), 3.02 (2H, d, $J = 21.3$ Hz), 2.97–2.77 (3H, m), 2.68 (1H, m), 2.48 (1H, dd, $J = 4.7, 15.0$ Hz), 2.22 (1H, m), 2.15 (1H, d, $J = 15.4$ Hz), 2.02 (1H, m), 1.94 (1H, m), 1.414 (3H, s), 1.407 (3H, s). FAB-MS (–VE) m/z 705 (M – H)[–]. HR-FAB-MS calcd for C₃₉H₄₂N₄O₉P (M – H)[–]: 705.268 94. Found: 705.268 96.

2-[(9S,10S,14S,18S)-7,16,19-Triaza-18-(carbamoylmethyl)-14-(naphthylmethyl)-8,17,20-trioxo-10-[4-(phosphonomethyl)phenyl]spiro[5.14]icos-11-en-9-yl]acetic Acid (6). Mp 260 °C (dec); ¹H NMR (CD₃OD) δ 8.64 (1H, s), 8.48 (1H, d, 7.9 Hz), 8.16 (1H, d, $J = 8.3$ Hz), 7.78 (1H, d, $J = 7.9$ Hz), 7.66 (1H, d, $J = 9.1$ Hz), 7.60 (1H, t, $J = 6.3$ Hz), 7.48 (1H, t, $J = 7.0$ Hz), 7.40 (1H, dd, $J = 6.9, 7.8$ Hz), 7.32 (2H, m), 7.22 (3H, m), 5.84 (1H, dd, $J = 11.1, 13.7$ Hz), 5.40 (1H, m), 4.49 (1H, m), 4.04 (1H, d, $J = 9.4$ Hz), 3.72 (1H, dd, $J = 6.7, 13.9$ Hz), 3.37 (2H, m), 3.02 (2H, d, $J = 21.7$ Hz), 2.96 (1H, dd, $J = 4.5, 15.2$ Hz), 2.88 (1H, m), 2.82 (1H, m), 2.68 (1H, dd, $J = 10.1, 13.8$ Hz), 2.45 (1H, dd, $J = 4.8, 15.2$ Hz), 2.28–1.90 (6H, m), 1.80 (2H, m), 1.58 (5H, m), 1.26 (1H, m); FAB-MS (–VE) m/z 745 (M – H)[–]; HR-FAB-MS calcd for C₃₉H₄₆N₄O₉P (M – H)[–]: 745.300 24. Found: 745.298 77.

Acknowledgment. This work was supported in part by a grant from the Susan G. Komen Breast Cancer Foundation to D.Y.

References

- Renhowe, P. A. Growth factor receptor kinases in cancer. *Annual Reports in Medicinal Chemistry*; Academic Press: London, 2001; pp 109–118.
- Wilkinson, S. E.; Harris, W. Selective tyrosine kinase inhibitors. *Emerging Drugs* **2000**, *5*, 287–297.
- Mendel, D. B.; Laird, A. D.; Smolich, B. D.; Blake, R. A.; Liang, C.; Hannah, A. L.; Shaheen, R. M.; Ellis, L. M.; Weitman, S.; Shawver, L. K.; Cherrington, J. M. Development of SU5416, a selective small molecule inhibitor of VEGF receptor tyrosine kinase activity, as an anti-angiogenesis agent. *Anti-Cancer Drug Des.* **2000**, *15*, 29–41.
- Noonberg, S. B.; Benz, C. C. Tyrosine kinase inhibitors targeted to the epidermal growth factor receptor subfamily: Role as anticancer agents. *Drugs* **2000**, *59*, 753–767.
- Levitzi, A. Protein tyrosine kinase inhibitors as therapeutic agents. *Top. Curr. Chem.* **2001**, *211*, 1–15.
- Ostman, A.; Heldin, C.-H. Involvement of platelet-derived growth factor in disease: Development of specific antagonists. *Adv. Cancer Res.* **2001**, *80*, 1–38.
- Pawson, T.; Gish, G. D.; Nash, P. SH2 domains, interaction modules and cellular wiring. *Trends Cell. Biol.* **2001**, *11*, 504–511.
- Shakespeare, W. C. SH2 domain inhibition: a problem solved? *Curr. Opin. Chem. Biol.* **2001**, *5*, 409–415.
- Muller, G. Peptidomimetic SH2 domain antagonists for targeting signal transduction. *Top. Curr. Chem.* **2001**, *211*, 17–59.
- Garcia-Echeverria, C. Antagonists of the Src homology 2 (SH2) domains of Grb2, Src, Lck and ZAP-70. *Curr. Med. Chem.* **2001**, *8*, 1589–1604.
- Fretz, H.; Furet, P.; Garcia-Echeverria, C.; Rahuel, J.; Schoepfer, J. Structure-based design of compounds inhibiting Grb2-SH2 mediated protein–protein interactions in signal transduction pathways. *Curr. Pharm. Des.* **2000**, *6*, 1777–1796.
- Rahuel, J.; Gay, B.; Erdmann, D.; Strauss, A.; Garcia-Echeverria, C.; Furet, P.; Caravatti, G.; Fretz, H.; Schoepfer, J.; Grutter, M. G. Structural basis for specificity of Grb2-SH2 revealed by a novel ligand binding mode. *Nat. Struct. Biol.* **1996**, *3*, 586–589.
- Garcia-Echeverria, C.; Gay, B.; Rahuel, J.; Furet, P. Mapping the X + 1 binding site of the Grb2-SH2 domain with alpha-alpha-disubstituted cyclic alpha-amino acids. *Bioorg. Med. Chem. Lett.* **1999**, *9*, 2915–2920.
- Furet, P.; Gay, B.; Caravatti, G.; Garcia-Echeverria, C.; Rahuel, J.; Schoepfer, J.; Fretz, H. Structure-based design and synthesis of high affinity tripeptide ligands of the Grb2-SH2 domain. *J. Med. Chem.* **1998**, *41*, 3442–3449.

- (15) Yao, Z. J.; King, C. R.; Cao, T.; Kelley, J.; Milne, G. W. A.; Voigt, J. H.; Burke, T. R., Jr. Potent inhibition of Grb2 SH2 domain binding by non-phosphate-containing ligands. *J. Med. Chem.* **1999**, *42*, 25–35.
- (16) Wei, C.-Q.; Li, B.; Guo, R.; Yang, D.; Burke, T. R., Jr. Development of a phosphatase-stable phosphotyrosyl mimetic suitably protected for the synthesis of high affinity Grb2 SH2 domain-binding ligands. *Bioorg. Med. Chem. Lett.* **2002**, *12*, 2781–2784.
- (17) Gao, Y.; Voigt, J.; Wu, J. X.; Yang, D.; Burke, T. R., Jr. Macrocyclization in the design of a conformationally constrained Grb2 SH2 domain inhibitor. *Bioorg. Med. Chem. Lett.* **2001**, *11*, 1889–1892.
- (18) Toniolo, C.; Benedetti, E. Old and new structures from studies on synthetic peptides rich in C-alpha, alpha-disubstituted glycines. *ISI Atlas Sci. Biochem.* **1988**, *1*, 225–230.
- (19) Toniolo, C.; Crisma, M.; Formaggio, F.; Valle, G.; Cavicchioni, G.; Precigoux, G.; Aubry, A.; Kamphuis, J. Structures of peptides from alpha-amino acids methylated at the alpha-carbon. *Biopolymers* **1993**, *33*, 1061–1072.
- (20) Gao, Y.; Wei, C.-Q.; Burke, T. R., Jr. Olefin metathesis in the design and synthesis of a globally constrained Grb2 SH2 domain inhibitor. *Org. Lett.* **2001**, *3*, 1617–1620.
- (21) Liu, D.-G.; Gao, Y.; Li, B.; Yang, D.; Burke, T. R., Jr. Synthesis of *N*-Fmoc 3-(4-(di-(*tert*-butyl)phosphonomethyl)phenyl)pipecolic acid as a conformationally constrained phosphotyrosyl mimetic suitably protected for peptide synthesis. *Tetrahedron*, submitted.
- (22) Miller, S. J.; Blackwell, H. E.; Grubbs, R. H. Application of ring-closing metathesis to the synthesis of rigidified amino acids and peptides. *J. Am. Chem. Soc.* **1996**, *118*, 9606–9614.
- (23) Phillips, A. J.; Abell, A. D. Ring-closing metathesis of nitrogen-containing compounds: applications to heterocycles, alkaloids, and peptidomimetics. *Aldrichimica Acta* **1999**, *32*, 75–89.
- (24) Furstner, A. Olefin metathesis and beyond. *Angew. Chem., Int. Ed.* **2000**, *39*, 3012–3043.
- (25) Burke, T. R., Jr.; Liu, D. G.; Gao, Y. Use of a Heck reaction for the synthesis of a new alpha-azido phosphotyrosyl mimetic suitably protected for peptide synthesis. *J. Org. Chem.* **2000**, *65*, 6288–6291.
- (26) Schwab, P.; France, M. B.; Ziller, J. W.; Grubbs, R. H. *Angew. Chem., Int. Ed. Engl.* **1995**, *34*, 2039–2041.
- (27) Scholl, M.; Ding, S.; Lee, C. W.; Grubbs, R. H. Synthesis and activity of a new generation of ruthenium-based olefin metathesis catalysts coordinated with 1,3-dimesityl-4,5-dihydroimidazol-2-ylidene ligands. *Org. Lett.* **1999**, *1*, 953–956.
- (28) Gao, Y.; Luo, J.; Yao, Z.-J.; Guo, R.; Zou, H.; Kelley, J.; Voigt, J. H.; Yang, D.; Burke, T. R., Jr. Inhibition of Grb2 SH2 domain binding by non-phosphate containing ligands. 2. 4-(2-Malonyl)phenylalanine as a potent phosphotyrosyl mimetic. *J. Med. Chem.* **2000**, *43*, 911–920.

JM0203635